Scientific Journal Widya Teknik
Volume 22 No. 1 2023
ISSN 1412-7350 eISSN 2621-362

THE EFFECT OF HYDROTHERMAL TREATMENT ON THE BIOLOGICAL PROPERTIES OF ANTING-ANTING (*ACALYPHA INDICA* LINN.) PLANT EXTRACT CONTAINING CARBON DOTS

Natasya Nadia Poetri Setiawaty, Jindrayani Nyoo Putro, Shella Permatasari Santoso*
Department of Chemical Engineering, Widya Mandala Surabaya Catholic University, Kalijudan 37, Surabaya 60114, Indonesia
*e-mail : shella@ukwms.ac.id

ABSTRACT

Anting-anting plant (Acalypha indica Linn.) is shrubs that grow as a weed in most parts of tropical countries. The plant has a record of ethno-pharmacological uses by native Asians, the plant has especially been used widely in the therapeutically practice in India. Owing to its rich biological active compounds content, Acalypha indica is rendered as a wild-plants with excellent antioxidant activities. In this work, hydrothermal extraction was performed to obtained liquid products containing high biological active compounds and carbon dots from Acalypha indica plant powder. The effect of hydrothermal temperature of 100, 110, 120, 130, and 140°C was evaluated on the optical properties and biological activity of the resultant liquid products from A. indica. The results imply that the liquid products obtained at highest investigated hydrothermal temperature of 140°C had the highest total phenolic and total flavonoid content, specifically the calculated total phenolic content is 5.50 mg GAE/g and total flavonoid content is 0.53 mg QE/g; that is higher than the non-hydrothermally treated extract. Owing to the high biological active compounds, the liquid products also show high radical scavenging activity, that is 78.5% against DPPH and 47.2% against superoxide radicals. The antibacterial assays show that the liquid product obtained from hydrothermal treatment at 140°C has better activity than the extract, with inhibition rate of 61.1 and 97.2% against Escherichia coli and Staphylococcus aureus, respectively.

ABSTRAK

Tanaman anting-anting (Acalypha indica Linn.) merupakan tumbuhan perdu yang tumbuh sebagai gulma di sebagian besar negara tropis. Tumbuhan ini memiliki catatan penggunaan etno-farmakologis oleh penduduk asli Asia, tumbuhan tersebut telah digunakan secara luas dalam praktik terapeutik di India. Karena kandungan senyawa aktif biologisnya yang kaya, Acalypha indica dianggap sebagai tanaman liar dengan aktivitas antioksidan yang potensial. Dalam penelitian ini, ekstraksi hidrotermal dilakukan untuk mendapatkan produk cair yang mengandung senyawa aktif biologis tinggi dan titik karbon dari bubuk tanaman Acalypha indica. Pengaruh suhu hidrotermal 100, 110, 120, 130, dan 140°C dievaluasi pada sifat optik dan aktivitas biologis produk cairan yang dihasilkan dari A. indica. Hasil penelitian menyiratkan bahwa produk cair yang diperoleh pada suhu hidrotermal tertinggi yang diselidiki 140 ° C memiliki kandungan total fenolik dan flavonoid total tertinggi, khususnya kandungan fenolik total yang dihitung adalah 5,50 mg GAE/g dan kandungan flavonoid total adalah 0,53 mg QE/g; yang lebih tinggi dari ekstrak yang tidak diolah secara hidrotermal. Karena kandungan senyawa aktif biologis yang tinggi, produk cair menunjukkan aktivitas penghilangan radikal yang tinggi, yaitu 78,5% terhadap DPPH dan 47,2% terhadap radikal superoksida. Uji antibakteri menunjukkan bahwa produk cair yang diperoleh dari perlakuan hidrotermal pada suhu 140°C memiliki aktivitas yang lebih baik daripada ekstrak, dengan tingkat penghambatan masing-masing sebesar 61,1 dan 97,2% terhadap Escherichia coli dan Staphylococcus aureus.

Keywords: *Carbon dots; Acalypha indica; Hydrothermal; Antioxidant; Antibacterial*

I. Introduction

Nanomaterial technology has been widely adopted in various field such as drug delivery system [1], pharmaceutical [2], wearable electronic device [3], water purification system [4], and many more. Hydrothermal procedure has been noted as a promising technique to release the water soluble organic compound from biomass. Hydrothermal technique is also considered as a green technology owing to the use of environmentally friendly solvent such as water. In this work, hydrothermal technique is used to produce liquid product from plant biomass which contain. Hydrothermal technique is typically performed at a temperature above water boiling point, the use of closed autoclave reactor allow the increase of pressure during the process. The increase of temperature and

pressure induce the auto-ionization of water and enhanced its solubility toward biomass, and the organic soluble compounds are extracted as the result. Furthermore, the high pressure during the reaction also facilitate the formation of carbon dots as the liquid product contain a high number of carbon-based compounds [5, 6].

Carbon dots can be conveniently synthesized from various carbon-containing compound, wherein, materials from nature always attract attention because of their renewable nature and abundance availability. Some example of carbon sources of carbon dots and their application is: citric acid for photodegradation of methyl blue [7], glucose for photo-electrochemical activity [8], and ammonium citrate as a histidine detector [9]. Besides purified-organic compounds, plants can also be utilized as the carbon soruces, e.g., Ginkgo leaves [10], broccoli [11], *Azadirachta indica* leaves [12], and *Catharanthus roseus* leaves [13]. The plant-based carbon source offers advantages such as inexpensive, high renewability and availability. Furthermore, utilization of plant as carbon dots starting materials can provide added value to the biomass [14].

Anting-anting (*Acalypha indica* Linn., abbreviated as *A. Indica* throughout this work) is a weed that grows in tropical areas such as Southeast Asia, including Indonesia. Indonesian people use *A. indica* as a medicine for cholesterol, rheumatism, and malaria; whose ability is induced by the antioxidant activity from the phytochemical content in *A. indica* [15]. So far, *A. indica* has only been used for traditional medication, and its use for advanced materials is still rare. In this study, *A. indica* was used as a carbon source in the preparation of liquid products containing carbon dots. *A. indica* contains protein and sugar, which high in carbon content; thus, convincing the potency of *A. indica* as raw or starting material for carbon dots [16].

The objectives in this work is producing the liquid products containing carbon dots through the hydrothermal treatment of *A. indica* plant extract. Temperature of the hydrothermal process is known to influenced the properties of the resulting liquid product, and therefore, the effect of hydrothermal temperature on the physical, optical, and biological activity of liquid products from *A. indica* was being evaluated. The characterization was carried out by means of spectrophotometric methods using Fourier transform infrared (FTIR) and UV-Vis technique. The biological properties of liquid products obtained from different hydrothermal temperatures was also evaluated, that is including the antioxidant properties and antibacterial properties.

II. Research methodology

II.1. Materials

Ethanol (C_2H_6O, 96%, Merck, USA), methanol (CH_4O, 95%, Sigma-Aldrich, USA), sodium carbonate (Na_2CO_3, Merck, USA), Folin-Ciocalteu reagent (Merck, USA), quercetin ($C_{15}H_{10}O_7$, 95%, Sigma-Aldrich, USA), aluminum chloride hexahydrate ($AlCl_3.6H_2O$, Ferak, Berlin), potassium acetate (CH_3COOK, Sigma-Aldrich, USA), acetic acid glacial (CH_3COOH, Merck, USA), and ammonium hydroxide (NH_4OH 25%, Merck, USA) was used for phytochemical assay in thi study. Bacterial culture of *Staphylococcus aureus* and *Eschericia coli*, nutrient agar (Merck, USA), nutrient broth (Merck, USA), chloramphenicol (Phapros, Indonesia), sulfuric acid (H_2SO_4, 95-97%, Merck, USA) and barium chloride ($BaCl_2.2H_2O$, Merck, USA) was used for antibacterial assay. DPPH ($C_{18}H_{12}N_5O_6$, Sigma-Aldrich, USA), trizma base ($C_4H_{11}NO_3$, Fluka), hydrochloric acid (HCl, 37%, Merck, USA), pyrogallol ($C_6H_6O_3$, Merck, USA) was used in antioxidant assay. *A. indica* (with 8% moisture) powder was obtained from a local shop in Surabaya, East Java, Indonesia. The solution used in this work was prepared by using deionized water. All of the chemicals were directly used as received without further treatment, unless otherwise noted.

II.2. Synthesis of liquid products

Three grams of *A. indica* powder were suspended in 75 mL of water in a Teflon autoclave. Subsequently, the autoclave was sealed and then put in an oven at specific temperature for five hours to initiate the hydrothermal reaction. The hydrothermal reaction was carried out at five different temperatures of 100, 110, 120, 130, and 140°C, and the corresponding liquid products were denoted as HTE_{100}, HTE_{110}, HTE_{120}, HTE_{130}, and HTE_{140}, respectively. The water was reduced from the liquid product to obtain concentrated solution by using rotary evaporator at 70°C, the concentrated extract has a volume of approximately quarter of the original volume (i.e., ±10 mL). The non-hydrothermal treated extract of *A. indica* (denoted as NTE) was also prepared by mercerizing the 3 g of plant powder in 75 mL of water at room temperature for 24h.

II.3. Phytochemical content assays

Prior for phytochemical assays of *A. indica* powder, 20 g of *A. indica* powder was added into 250 mL of water. The *A. indica* extract was obtained through maceration technique, where the *A. indica* suspension was left to stand for 24 hours at room temperature. The extract was separated from the solids using a centrifuge at 6000 rpm for 5 minutes. The water was reduced from the extract to obtain concentrated extract by using rotary evaporator

at 70°C, the concentrated extract has a volume of quarter of the original volume (i.e., ±10 mL). For HTEs samples, the concentrated HTEs solution was directly used, at certain dilution ratio, prior to the assays. The phytochemical content was evaluated according to total phenolic content (TPC) and total flavonoid content (TFC), all of the measurements were done in duplicate.

II.3.1. TPC

The TPC was determined using Folin-Ciocalteu (FC) reagent. A series of gallic acid solution was prepared at concentration of 2, 4, 6, 8, and 10 ppm. Into 2 mL of the gallic acid solution, 6 mL of 10% FC reagent and 12 mL of 7.5% Na_2CO_3 solution were added. Then, the mixture was kept for 1 hour in a dark environment. The absorbance of solutions was measured with a UV-Vis spectrophotometer at a wavelength of 737 nm. The TPC is expressed as mg gallic acid equivalent (GAE)/g sample [17].

II.3.2. TFC

A series of quercetin solution at concentration of 20, 40, 60, 80, and 100 ppm was prepared. 1 mL of the quercetin solution was then mix with 1 mL of 2% $AlCl_3$ solution and 1 mL of 120 mM CH_3COOK solution. Then, the mixture was stored for 1 hour at room temperature. The absorbance of the solutions was measured with a UV-Vis spectrophotometer at a wavelength of 425 nm. The TFC is expressed as mg quercetin equivalent (QE)/g sample [17].

II.4. Characterization of CQDs

The functional groups of HTEs were analyzed using FTIR method on a Shimadzu FTIR-8400S infrared spectrophotometer. The UV-Vis absorption spectra of HTEs was measured using a Shimadzu UV-1700 UV-Vis Spectrophotometer.

II.5. Antioxidant assay

The biological activity of NTE and HTEs was determined as the antioxidant and antibacterial activity. The antioxidant activity was tested against DPPH [19] and superoxide [20]. Meanwhile, the antibacterial activity was determined against *Staphylococcus aureus* (*S. aureus*) and *Eschericia coli* (*E. coli*) by employing disc diffusion [21] and plate count [22] methods.

II.5.1. DPPH assay

DPPH solution with a concentration of 100 ppm was prepared in a dark-colored bottle. 2 mL of of DPPH solution was then added into 2 mL of tested sample, and then allowed to stand for 30 minutes in the dark. Then the absorbance was measured using a UV-Vis spectrophotometer at a wavelength of 517 nm. Prior to the assay, a blank solution consisted of 2 ml of distilled water and 2 ml of DPPH solution was prepared and measured. The %DPPH inhibition was calculated as:

$$\%\text{DPPH inhibition} = (A_{blank}-A_{sample})/A_{blank}\times 100 \quad (1)$$

where A_{blank} and A_{sample} represent the absorbance of the blank solution and the sample, respectively.

II.5.2. Superoxide assay

50 mM Tris-HCl buffer solution with a pH of 8.2, 3 mM pyrogallol solution, and 10 mM HCl solution was prepared prior to the assay. Then, 0.2 mL of sample was added into 5.7 mL Tris-HCl buffer solution and then being incubated for 20 minutes at room temperature. Then 0.1 mL of 3 mM pyrogallol solution was added, and the mixture was further incubated for 5 minutes at room temperature. Into the mixture, 0.1 mL of 10 mM HCl solution was added. The absorbance was measured with a UV-Vis spectrophotometer at a wavelength of 320 nm. Blank solutions were prepared in the same order without the addition of the sample. The %superoxide radical scavengers (%SRS) was calculated as follow:

$$\%\text{SRS} = (A_{blank}-A_{sample})/A_{blank}\times 100 \quad (2)$$

II.5.3. Disc diffusion method

Muller-Hinton agar (MHA) plates were prepared in advance prior for the disc diffusion assay. *S. aureus* or *E. coli* suspension was prepared at concentration of 1.5×10^8 CFU/mL, which is equivalent to 0.5 McFarland standard. Each of bacteria suspension was evenly smeared on MHA using a sterile cotton swab. The MHA plate was divided into four areas with equal size, the areas were designated for (1) distilled water (negative control), (2) chloramphenicol (positive control), (3) NTE, and (4) HTEs. Then, the prepared paper disc was dipped into each of the designated samples and put on the bacteria-smeared MHA. The plates were incubated at 37°C for 24 hours.

II.5.4. Plate count method

From a 1.5×10^8 CFU/mL (equivalent to 0.5 McFarland standard) *E. coli* or *S. aureus* bacterial suspensions, diluted bacterial suspension at concentration of 1.5×10^2 CFU/mL was prepared. 1 mL of the tested sample was then added into the diluted and then incubated at 37°C for 24 hours. Subsequently, six times serial dilution with a factor of 10 was prepared from the incubated sample. Then, 0.1 mL of each dilution was plated on nutrient agar and incubated at 37°C for 16 hours. After incubation, the number of colonies forming units (CFU) was counted.

III. Research results and discussions

III.1. Total phenolic and flavonoid content

Hydrothermal treatment was imposed for the extraction of biological active compound from *A. indica*, various hydrothermal temperatures of 100, 110, 120, 130, and 140°C were used for the process and resulting in

HTE_{100}, HTE_{110}, HTE_{120}, HTE_{130}, and HTE_{140}, respectively. As shown in the Scheme 1, the apparent physical phenomena that could be observed during the hydrothermal treatment is the change of turbid and muddies-colored *A. indica* suspension into transpicuous-brown colored solution. Hydrothermal treatment involving the water molecules to induce disruption on the hydrogen bonds of plant tissues and facilitate the release of organic compounds.

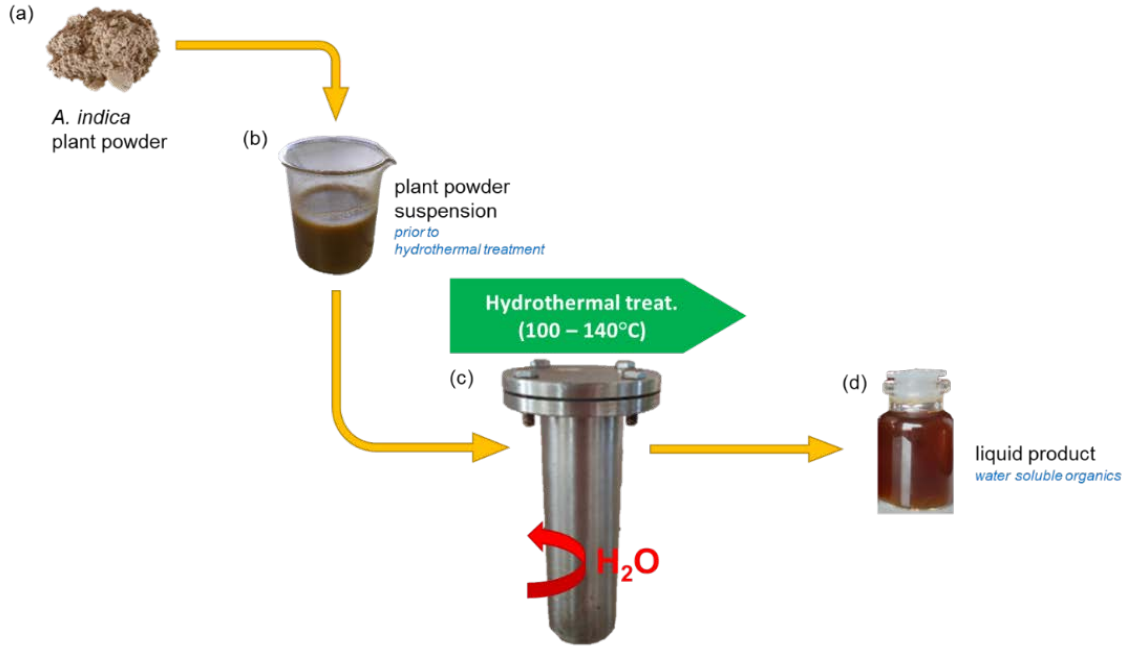

Scheme 1. Hydrothermal treatment of *A. indica* to produce liquid product containing water soluble organics. (a) Dried plant powder, (b) suspension of plant powder in water, (c) hydrothermal treatment using autoclave, and (d) resultant liquid product from hydrothermal treatment.

The sum of phenolic compounds in the extract was calculated as the total phenolic content (TPC), Fig. 1 shows the effect of hydrothermal treatment on the TPC. A decreased in TPC was observed with an increase of hydrothermal temperature from 100°C to 120°C, the computed TPC for HTE_{100}, HTE_{110}, and HTE_{120} is 3.24, 3.21, and 2.57 mg GAE/g, respectively —These TPC values was found to be lower than the non-hydrothermal treated extract (NTE) with TPC of 3.82 mg GAE/g. Interestingly, the TPC was found to increase as the hydrothermal temperature was further increased to 130°C and 140°C, with TPC value for HTE_{130} and HTE_{140} is 4.23 and 5.50 mg GAE/g, respectively; which is notably higher than NTE.

The sum of flavonoid of the plant extract was calculated as the total flavonoid content (TFC). A similar decreasing-increasing pattern of TFC and TPC values was observed. As shown in Fig. 1, the TFC was found to decrease during the hydrothermal treatment with temperature of 100, 110, and 120°C; the TFC content is 0.39, 0.40, 0.35 mg QE/g for HTE_{100}, HTE_{110}, and HTE_{120}, respectively, that is lower than the NTE with TFC value of 0.43 mg QE/g. A significant increase of TFC, higher than NTE, was noted for hydrothermal treated extract at temperature of 130 and 140°C; specifically, the calculated TFC value is 0.46 and 0.53 mg QE/g for HTE_{130} and HTE_{140}, respectively.

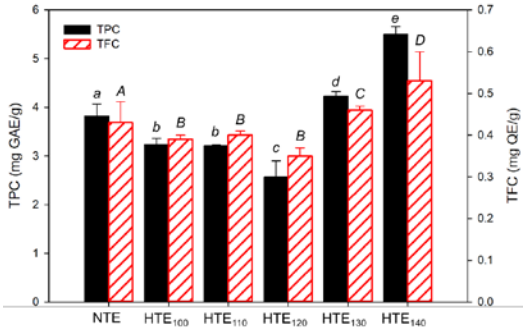

Figure 1. TPC and TFC of *A. indica* extracts treated at different hydrothermal temperature. Different letters indicate significant different.

Hydrothermal treatment is expected to intensify the phenolic and flavonoid compound release from the plant. However, according to the computed results, hydrothermal temperature of 100–120°C resulted in extract with poor TPC and TFC compared to the non-treated extract NTE. This can be correlated to the supercritical condition achievement during the hydrothermal process, at the temperature of 100–120°C, the pressure inside the autoclave might be fall below the critical point of water solvent; the actual pressure of the system was not able to measure from the apparatus used in this work. As the sub- or supercritical condition was not

reach, thermal breakdown of the phytochemicals was probably occurred instead [24-26]. Meanwhile, for HTE_{130} and HTE_{140} which treated at temperature of 130 and 140°C has higher TPC and TFC than NTE. In this case, the sub- or supercritical condition might be achieved and increasing the solubility of the solvent against organic components [24, 27]. The high water solubility of organic components during this stage occurs due to the increase intermolecular collisions which lead to the weakening of hydrogen bonds and increasing the dipole moment force [28]. Subsequently, the polarity of water decrease and be able to dissolve more of the organic components.

III.2. Spectroscopy measurement

The qualitative assay on the fluorescence property of NTE and HTEs was observed by irradiating the diluted solution (solid-to-water ratio 1:11) with UV light at wavelength of 366 nm. As given in Fig. 2, the HTEs solution give more apparent bluish light emission than that of NTE, suggesting the conversion of some carbon content into carbon dots, similar phenomenon was reported by Yang et al. [29]. The blue light emission occurs due to a surface defect caused by the hybridization of sp^2, sp^3 carbon, and oxygen functional groups on the surface [30, 31]. Carbon dots are basically carbon and have the electron configuration of $(1s^2)2s^22p^2$, the electrons in the ground state absorb energy from the UV light and causing their excitation to a higher orbital level. Electrons vibration relaxation was then occurred and return back the electrons to the ground state [32]. The electron movements take place at the π and π^* energy levels of the sp^2 carbon, which is confined to the bandgap between the σ and σ^* energy levels of the sp^3 carbon, which is in accordance to the nanomaterials theory or quantum confinement effect [6, 21].

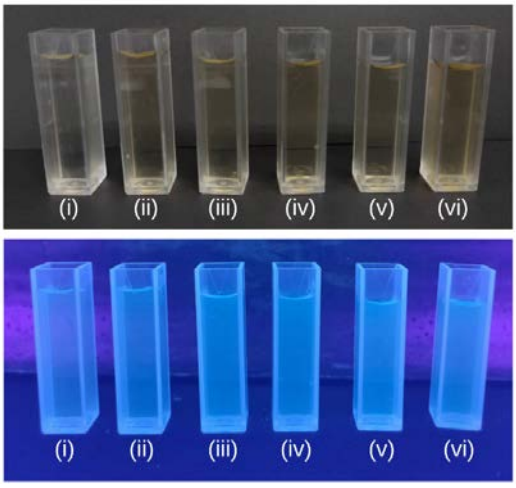

Figure 2. The appearance of the solution without UV light irradiation (up) and blue light emission of the extract as irradiated with UV at 366 nm (down). The sample number: (i) NTE, (ii) HTE_{100}, (iii) HTE_{110}, (iv) HTE_{120}, (v) HTE_{130}, and (vi) HTE_{140}.

The UV-Vis absorbance pattern of HTEs on the effect of different hydrothermal temperatures was measured at wavelength of 200-800 nm, and the result is provided in Fig. 3a, the inset figure shows the enlarged graphic at 200-400 nm. All of the HTEs sample was prepared at the same concentration at 3.25 mg/mL. It can be noted that HTE_{140} exhibits higher light absorption and resulted at higher intensity than other samples, which can be correlated to the higher number of carbon dots present in the liquid product. Several distinguishable band was observed to occur in the spectra. Specifically the absorbance at 280 nm corresponding to the π-π^* transition of the C=C group [21, 35] was able to observe for HTE_{100} and HTE_{110}. It can be noted that the band at 280 nm is shifted to lower wavelength for other sample which extracted at higher hydrothermal temperature, i.e., the band shifted to 271 in HTE_{140}. This can be ascribed to the more homogeneous size distribution of the resulting carbon-dots nanoparticles [33, 34]. The appearance of peak at 342 nm which only noted for HTE_{140} indicates the n-π^* transition of the C=O group, the appearance of this peak also indicates the oxidation occurred during the hydrothermal reaction [29, 36].

Furthermore, the blue shift of the band from 280 nm to 271 nm is correlated to the particle size and distribution [37]; according to the quantum confinement theory, smaller particles result in a lower maximum wavelength shift or blue shift [38, 39]. The smaller the particle size, the greater the bandgap between the highest occupied molecular orbital (HOMO) and the lowest unoccupied molecular orbital (LUMO) will be [40]. Therefore, higher energy is required to cause the excitation of electrons, which lead to the lower the absorption wavelength [41, 42]. To further evaluate the effect of number of carbon dots on the wavelength shift, the UV-Vis spectra of HTE_{140} at different concentration was measured and the result is shown in Fig. 4b. It can be seen that the absorbance intensity increases as the concentration of carbon dots in HTE_{140} increases.

Scientific Journal Widya Teknik
Volume 22 No. 1 2023
ISSN 1412-7350 eISSN 2621-362

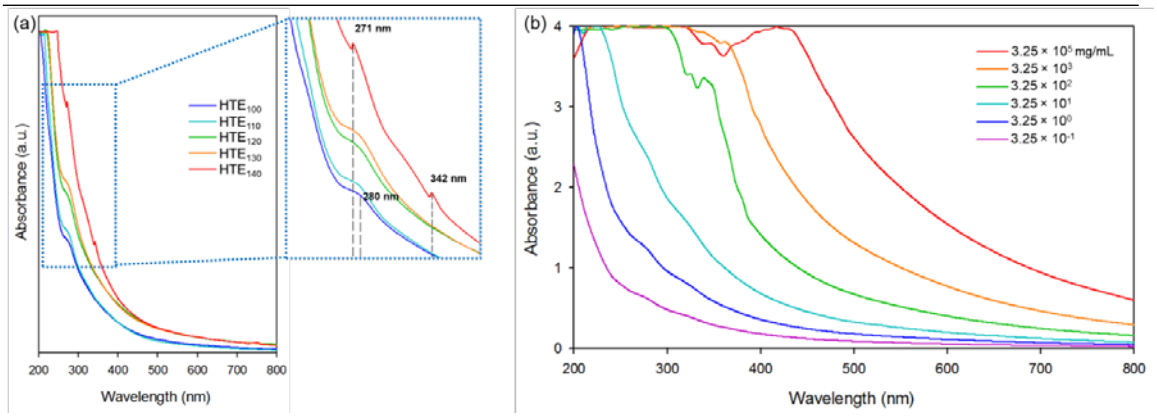

Figure 3. UV-Vis spectrum pattern of HTEs: (a) the pattern for HTEs synthesized at different hydrothermal temperatures, and (b) the pattern of HTE_{140} at different dilution concentration.

III.3. FTIR characterization

FTIR characterization was carried out on freeze dried HTE_{140} to evaluate the functional groups, the FTIR spectra is presented in Fig. 4. The absorbance peak at 890 cm^{-1} is corresponding to the out-of-plane bending of C─H bond [43]. The peak at 1039 and 1387 cm^{-1}, respectively, correspond to the stretching of carboxylate moieties of C─O and COO─ [44, 45]. The peak at 1653 cm^{-1} is related to C=O stretching [46]. The peak at 2359 cm^{-1} is corresponding to the stretching to C-N bond [35]. The peak at 2943 cm^{-1} can be correlated to C─H bond of CH_3 group [47]. The broad absorbance peak at 3242 cm^{-1} can be attributed to the stretching vibration of O─H group [48].

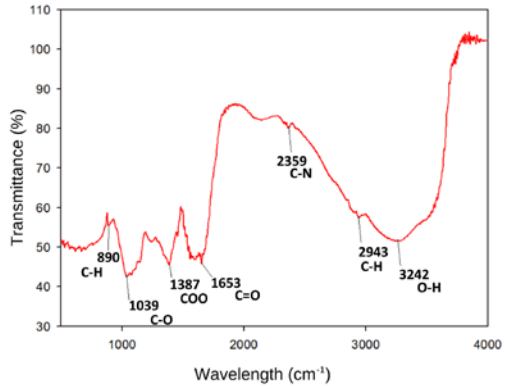

Figure 4. FTIR spectrum of HTE_{140}.

III.4. Biological activity assays

III.4.1. Radical scavenging activity

DPPH antioxidant assay is a method that uses the DPPH radical, which is very stable, and does not react to oxygen [49]. The DPPH inhibition activity of the NTE and HTEs was evaluated and the result is presented in Table 1. It can be noted that each HTEs sample exhibit different DPPH inhibitory activity, indicating that the hydrothermal temperature affects the anti-oxidative properties of HTEs. The HTEs obtained from hydrothermal treatment temperature of 100, 110, and 120°C show lower DPPH inhibition compared to the NTE. Meanwhile, the HTEs obtained from hydrothermal treatment at higher temperature of 130 and 140°C shows more excellent DPPH inhibition to that of *A. indica* extract.

The reactive oxygen species in the form of superoxide radical (O_2^-), which is naturally produced from the cell [50], was used to evaluate the inhibition activity of the samples against the superoxide radical. These radicals are dangerous because they can cause oxidative stress by damaging DNA, lipids, and proteins in cells [51], which can potentially cause various serious diseases [52]. The superoxide radical scavenging activity of each sample is also presented in Table 1. It can be noted that the superoxide radical inhibition was lower than NTE for HTE_{100}, HTE_{110}, and HTE_{120}; meanwhile, HTE_{130} and HTE_{140} show a comparable or higher superoxide radical inhibition than that of NTE.

Table 1. Radical inhibitory activity of HTEs

Sample	%inhibition	
	DPPH	Superoxide
NTE	78.0 ± 0.12[a]	43.1 ± 1.12[a]
HTE_{100}	73.1 ± 3.21[b]	33.8 ± 2.31[b]
HTE_{110}	69.2 ± 0.02[b]	30.5 ± 0.11[b]
HTE_{120}	58.5 ± 0.55[c]	34.8 ± 0.78[b]
HTE_{130}	**85.8 ± 0.78[d]**	44.2 ± 0.21[a]
HTE_{140}	78.5 ± 1.23[a]	**47.2 ± 0.57[c]**

Different letter represent a significant difference ($P < 0.05$) relative to the NTE

The above results denoted that HTEs obtained from hydrothermal treatment at a temperature of 100–120°C had lower antioxidant activity than NTE, this can be ascribed to the lower phytochemical content of the samples as noted from their calculated TPC and TFC (see Fig. 1). On the other hand, the hydrothermal treatment at higher temperature of 130 and 140°C in producing HTE_{130} and HTE_{140} allows the formation of oxygenated functional

groups [54, 30], as indicated by the presence of a C=O group bond (see FTIR spectra in Fig. 4). The oxygenated functional groups act as electron donor to neutralize free radicals from DPPH and superoxide anions [55], the radical scavenging mechanism is illustrated in Fig. 5.

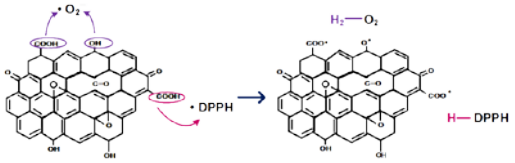

Figure 5. DPPH and superoxide radical scavenging mechanism by HTEs.

III.4.2. Antibacterial activity

Table 2 shows the inhibition zones of NTE and HTEs against investigated bacteria strain. It can be noted that NTE and HTEs show low (or no) inhibitory power against gram-negative bacteria *Escherichia coli*; but, NTE and HTEs exhibit a potential inhibitory activity on gram-positive bacteria *Staphylococcus aureus*; which indicated by the higher inhibition zone diameters. Quantification on the inhibition rate of the samples was performed by utilizing the standard plate count method, and the results presented in Table 3. It can be noted that the inhibition rates of NTE and HTEs were significantly lower for the gram-negative bacteria *Escherichia coli* than that of against gram-positive bacteria *Staphylococcus aureus*. The effect of hydrothermal temperature can also be noted from the inhibition rate in Table 3, HTEs which synthesized at higher temperature of 130 and 140°C show greater antibacterial activity than NTE, which can be due to the higher TFC and TPC content and the effect of reducing carbon dots particle size [56].

Table 2. Inhibition zones of HTEs against gram-positive and gram-negative bacteria

Bacteria	**Inhibition zone [b] (mm)**						
	Positive control [a]	NTE	HTE_{100}	HTE_{110}	HTE_{120}	HTE_{130}	HTE_{140}
E. coli	12	–	–	–	–	–	3
S. aureus	16	2	4	5	5	5	7

[a] Chloramphenicol
[b] (–) = no inhibtion zone

Table 3. Inhibition rate of HTEs against gram-positive and gram-negative bacteria

Sample	**Bacteria**			
	E. coli		***S. aureus***	
	Number of colonies (CFU/mL)	**Inhibition rate (%)**	**Number of colonies (CFU/mL)**	**Inhibition rate (%)**
Control	1.8×10^{9}	–	3.0×10^{10}	–
NTE	1.6×10^{9}	11.11	2.5×10^{10}	16.70
HTE_{100}	1.3×10^{9}	25.93	2.1×10^{9}	93.05
HTE_{110}	1.4×10^{9}	22.22	1.9×10^{9}	93.50
HTE_{120}	1.3×10^{9}	25.93	1.3×10^{9}	95.74
HTE_{130}	1.2×10^{9}	31.48	1.3×10^{9}	95.74
HTE_{140}	7.0×10^{8}	61.11	8.3×10^{8}	97.20

The hydrothermal temperature has a significant effect on the antibacterial activity of the HTEs. The higher synthesize temperature is resulted in HTEs with better antibacterial activity, which can be ascribed to the effect of particle size and distribution. The smaller the particle size, the easier it is to penetrate the structure of the bacterial cell wall so that the antibacterial ability produced is maximized [56], further study on evaluating the specific size of the carbon dots in HTEs should be performed to confirm the phenomena. Furthermore, the better antibacterial activity of HTEs treated at higher hydrothermal temperature can be correlated to the higher TPC and TFC. Phenolic components, including flavonoids, are compounds that have hydroxyl bonds in their phenol groups [57], these groups can inhibit the bacterial growth owing to their high binding affinity to proteins on enzymes in microbes and cytoplasmic membranes [58]. Enzymes in microbes, such as penicillin-binding protein, are involved in synthesizing peptidoglycan, which is a component of the bacterial cell wall [59]; by interfering with the work of these enzymes, bacterial growth can be inhibited.

The better antibacterial activity of HTEs against the gram-positive bacteria than the gram-negative bacteria can be correlated to the cell wall structure of the bacteria. The gram-positive bacteria has more simple cell wall composition, that is thick layer of peptidoglycan containing teichoic and lipoteichoic acids and a porous cell wall [60, 61]. Meanwhile, gram-negative bacteria have a more complex cell wall structure, with a thin peptidoglycan layer between the cytoplasmic and outer membranes. The complexity of the membrane layer containing lipids, proteins, and lipopolysaccharides (LPS) provides resistance to antibacterial agents [61, 62]. The lipids and

lipopolysaccharides of gram-negative bacteria has lipophilic nature [63], on the other hand, carbon dots in HTEs are nanomaterials with high solubility in water ―The different lipophilicity between HTEs and cell wall of bacteria may induce interference of HTEs to penetrate into the cell wall.

IV. Conclusion

Liquid product from weed plant *Acalypha indica* Linn. (aka. Anting-anting plant) were successfully obtained through hydrothermal treatment of water extract of the plant powder. The use of water as the solvent denotes the environmentally friendly method which can be used to promote the green and sustainable technology. The present work demonstrated the effect of hydrothermal treatment temperature on the properties and biological activities of the resulting liquid products, wherein higher hydrothermal temperature results in liquid product with better properties. Specifically, hydrothermal temperature of 140°C was found to be the best condition for producing liquid product with high TPC and TFC, excellent antioxidant and antibacterial activity. Further study should be subjected to evaluate the organic composition of the liquid product to identify the active compounds responsible for the biological activities. Furthermore, to reveal the carbon dots in the liquid products, transmission electron microscopy analysis should be performed to determine the particle size.

References

1. Zhou, J., Meng, L., Sun, C., Ye, W., Chen, C., Du, B., "A "protective umbrella" nanoplatform for loading ICG and multi-modal imaging-guided phototherapy" *Nanomedicine* 2018, **14**, 289–301.
2. Benrabah, L., Kemel, K., Twarog, C., Huang, N., Solgadi, A., Laugel, C., Faivre, V., "Lipid-based Janus nanoparticles for pharmaceutical and cosmetic applications: Kinetics and mechanisms of destabilization with time and temperature" *Colloids Surf. B* 2020, **195**, 111242.
3. Zhou, Y., Wu, S., Liu, F., "High-performance polyimide nanocomposites with polydopaminecoated copper nanoparticles and nanowires for electronic applications" *Mater. Lett.* 2019, **237**, 19-21.
4. Mittal, A., Mittal, J., Malviya, A., Gupta, V.K., "Removal and recovery of Chrysoidine Y from aqueous solutions by waste materials" *J. Colloid Interface Sci.* 2010, **344**, 497–507.
5. Wang, Y.,Hu, A., "Carbon quantum dots: synthesis, properties and applications" *J. Mater. Chem. C* 2014, **2**, 6921-6939.
6. Lim, S.Y., Shen, W., Gao, Z., "Carbon quantum dots and their applications" *Chemical Society Reviews* 2015, **44**, 362-381.
7. Aghamali, A., Khosravi, M., Hamishehkar, H., Modirshahla, N., Behnajady, M.A., "Synthesis and characterization of high efficient photoluminescent sunlight driven photocatalyst of N-Carbon Quantum Dots" *J. Lumin.* 2018, **201**, 265-274.
8. Xie, X., Yang, Y., Xiao, Y.-H., Huang, X., Shi , Q., Zhang , W.-D., "Enhancement of photo-electrochemical activity of Fe_2O_3 nanowires decorated with carbon quantum dots" *Int. J. Hydrog. Energy* 2018, **43**, 6954-6962.
9. Che, Y., Pang, H., Li, H., Yang, L., Fu, X., Liu, S., Ding, L., Hou, J., "Microwave-assisted fabrication of copper-functionalized carbon quantum dots for sensitive detection of histidine" *Talanta* 2019, **196**, 442-448.
10. Jiang, X., Qin, D., Mo, G., Feng, J., Yu, C., Mo, W., Deng, B., "Ginkgo leaf-based synthesis of nitrogen-doped carbon quantum dots for highly sensitive detection of salazosulfapyridine in mouse plasma" *J. Pharm. Biomed.* 2019, **164**, 514–519.
11. Arumugam, N.,Kim, J., "Synthesis of carbon quantum dots from Broccoli and their ability to detect silver ions" *Mater. Lett.* 2018, **219**, 37-40.
12. Yadav, P.K., Singh, V.K., Chandra, S., Bano, D., Kumar, V., Talat, M., Hasan, S.H., "Green Synthesis of Fluorescent Carbon Quantum Dots from Azadirachta indica Leaves and Their Peroxidase-Mimetic Activity for the Detection of H_2O_2 and Ascorbic Acid in Common Fresh Fruits" *ACS Biomater. Sci. Eng.* 2019, **5**, 623-632.
13. Arumugham, T., Alagumuthu, M., Amimodu, R.G., Munusamy, S., Iyer, S.K., "A sustainable synthesis of green carbon quantum dot (CQD) from *Catharanthus roseus* (white flowering plant) leaves and investigation of its dual fluorescence responsive behavior in multi-ion detection and biological applications" *SM&T* 2020, **23**, e00138.
14. Zhang, X., Jiang, M., Na, N., Chen, Z., Li, S., Liu, S., Li, J., "Review of natural product derived carbon dots: from natural products to functional materials" *ChemSusChem* 2018, **11**, 11-24.
15. Silalahi, M., "*Acalypha Indica*: Pemanfaatan dan Bioaktivitasnya" *Titian Ilmu: Jurnal Ilmiah Multi Sciences* 2019, **11**, 81-86.
16. Umate, S.K.,Marathe, V.R., "Nutraceutical evaluation of Acalypha indica L.-A potential wild edible plant" *Int. J. Green Pharm.* 2018, **12**, S510.
17. Al-Owaisi, M., Al-Hadiwi, N., Khan, S.A., "GC-MS analysis, determination of total phenolics, flavonoid content and free radical scavenging activities of various crude extracts of Moringa peregrina (Forssk.) Fiori leaves" *Asian Pac. J. Trop. Biomed.* 2014, **4**, 964-970.

18. Muthukrishnan, S.,Manogaran, P., "Phytochemical analysis and free radical scavenging potential activity of Vetiveria zizanioides Linn" *J. Pharmacogn. Phytochem.* 2018, **7**, 1955-60.
19. Huang, G., Lin, Y., Zhang, L., Yan, Z., Wang, Y., Liu, Y., "Synthesis of sulfur-selenium doped carbon quantum dots for biological imaging and scavenging reactive oxygen species" *Sci. Rep.* 2019, **9**, 1-9.
20. Chen, K., Qing, W., Hu, W., Lu, M., Wang, Y., Liu, X., "On-off-on fluorescent carbon dots from waste tea: Their properties, antioxidant and selective detection of CrO42−, Fe3+, ascorbic acid and L-cysteine in real samples" *Spectrochim. Acta A Mol. Biomol. Spectrosc.* 2019, **213**, 228-234.
21. Shahshahanipour, M., Rezaei, B., Ensafi, A.A., Etemadifar, Z., "An ancient plant for the synthesis of a novel carbon dot and its applications as an antibacterial agent and probe for sensing of an anti-cancer drug" *Materials Science & Engineering C* 2019, **98**, 826–833.
22. Bankier, C., Cheong, Y., Mahalingam, S., Edirisinghe, M., Ren, G., Cloutman-Green, E., Ciric, L., "A comparison of methods to assess the antimicrobial activity of nanoparticle combinations on bacterial cells" *PLoS One* 2018, **13**, e0192093-e0192093.
23. Lencova, S., Zdenkova, K., Jencova, V., Demnerova, K., Zemanova, K., Kolackova, R., Hozdova, K., Stiborova, H., "Benefits of Polyamide Nanofibrous Materials: Antibacterial Activity and Retention Ability for Staphylococcus Aureus" *Nanomaterials* 2021, **11**, 480.
24. Shiddiqi, Q.Y.A., Karisma, A.D., Machmudah, S., Widiyastuti, W., Nurtono, T., Winardi, S., Wahyudiono, W., Goto, M., "Effect of hydrothermal extraction condition on the content of phenolic compound extracted from rind of mangosteen (*Garcinia mangostana*) and its antioxidant efficiency" *J. IPTEK-KOM* 2015, **25**.
25. Ong, E.S., Cheong, J.S.H., Goh, D., "Pressurized hot water extraction of bioactive or marker compounds in botanicals and medicinal plant materials" *J. Chromatogr. A* 2006, **1112**, 92-102.
26. Ghafoor, K., Ahmed, I.A.M., Doğu, S., Uslu, N., Fadimu, G.J., Al Juhaimi, F., Babiker, E.E., Özcan, M.M., "The effect of heating temperature on total phenolic content, antioxidant activity, and phenolic compounds of plum and mahaleb fruits" *Int. J. Food Eng.* 2019, **15**.
27. Ayala, R.S.,De Castro, M.L., "Continuous subcritical water extraction as a useful tool for isolation of edible essential oils" *Food Chem.* 2001, **75**, 109-113.
28. Plaza, M.,Marina, M.L., "Pressurized hot water extraction of bioactives" *TrAC - Trends in Analytical Chemistry* 2019, **116**, 236-247.
29. Yang, Q., Duan, J., Yang, W., Li, X., Mo, J., Yang, P., Tang, Q., "Nitrogen-doped carbon quantum dots from biomass via simple one-pot method and exploration of their application" *Appl. Surf. Sci.* 2018, **434**, 1079-1085.
30. Lim, S.Y., Shen, W., Gao, Z., "Carbon quantum dots and their applications" *Chem. Soc. Rev.* 2015, **44**, 362-381.
31. Lin, L., Rong, M., Lu, S., Song, X., Zhong, Y., Yan, J., Wang, Y., Chen, X., "A facile synthesis of highly luminescent nitrogen-doped graphene quantum dots for the detection of 2,4,6-trinitrophenol in aqueous solution" *Nanoscale* 2015, **7**, 1872-1878.
32. Lichtman, J.W.,Conchello, J.-A., "Fluorescence microscopy" *Journal Nature methods* 2005, **2**, 910-919.
33. Haiss, W., Thanh, N.T., Aveyard, J., Fernig, D.G., "Determination of size and concentration of gold nanoparticles from UV−Vis spectra" *J. Anal. Chem.* 2007, **79**, 4215-4221.
34. Costa, L., Hemmer, J., Wanderlind, E., Gerlach, O., Santos, A., Tamanaha, M., Bella-Cruz, A., Corrêa, R., Bazani, H., Radetski, C., "Green synthesis of gold nanoparticles obtained from algae Sargassum cymosum: optimization, characterization and stability" *J. Bionanosci.* 2020, **10**, 1049-1062.
35. Sachdev, A.,Gopinath, P., "Green synthesis of multifunctional carbon dots from coriander leaves and their potential application as antioxidants, sensors and bioimaging agents" *Analyst* 2015, **140**, 4260-4269.
36. Rani, U.A., Ng, L.Y., Ng, C.Y., Mahmoudi, E., "A review of carbon quantum dots and their applications in wastewater treatment" *Advances in Colloid and Interface Science* 2020, **278**, 102124.
37. Wu, Q., Li, W., Wu, P., Li, J., Liu, S., Jin, C., Zhan, X., "Effect of reaction temperature on properties of carbon nanodots and their visible-light photocatalytic degradation of tetracyline" *RSC advances* 2015, **5**, 75711-75721.
38. Yang, L., Reed, D., Adu, K.W., Arriaga, A.L.E., "Quantum Confinement Effect in the Absorption Spectra of Graphene Quantum Dots" *MRS Adv.* 2019, **4**, 205-210.
39. Vatankhah, C., Saki, M., Jafargholinejad, S., "Theoretical and experimental investigation of quantum confinement effect on the blue shift in semiconductor quantum dots" *Orient. J. Chem* 2015, **31**, 907-912.
40. Rabouw, F.T.,de Mello Donega, C., *Excited-State Dynamics in Colloidal Semiconductor Nanocrystals*, in *Photoactive Semiconductor Nanocrystal Quantum Dots: Fundamentals and Applications*, Credi, A.,

Editor. 2017, Springer International Publishing: Cham. p. 1-30.
41. Britto-Hurtado, R.,Cortez-Valadez, M., *Chapter 4 - Green synthesis approaches for metallic and carbon nanostructures*, in *Green Functionalized Nanomaterials for Environmental Applications*, Shanker, U., Hussain, C.M., and Rani, M., Editors. 2022, Elsevier. p. 83-127.
42. He, M., Zhang, J., Wang, H., Kong, Y., Xiao, Y., Xu, W., "Material and Optical Properties of Fluorescent Carbon Quantum Dots Fabricated from Lemon Juice via Hydrothermal Reaction" *Nanoscale Res Lett* 2018, **13**, 175-175.
43. Gan, Z., Wu, X., Hao, Y., "The mechanism of blue photoluminescence from carbon nanodots" *CrystEngComm* 2014, **16**, 4981-4986.
44. Wu, J., Wang, P., Wang, F., Fang, Y., "Investigation of the microstructures of graphene quantum dots (GQDs) by surface-enhanced Raman spectroscopy" *Nanomaterials* 2018, **8**, 864.
45. Kondratenko, T., Ovchinnikov, O., Grevtseva, I., Smirnov, M., Erina, O., Khokhlov, V., Darinsky, B., Tatianina, E., "Thioglycolic Acid FTIR Spectra on Ag_2S Quantum Dots Interfaces" *Materials* 2020, **13**, 909.
46. Nasseri, M.A., Keshtkar, H., Kazemnejadi, M., Allahresani, A., "Phytochemical properties and antioxidant activity of Echinops persicus plant extract: green synthesis of carbon quantum dots from the plant extract" *SN Appl. Sci.* 2020, **2**, 670.
47. Janus, Ł., Radwan-Pragłowska, J., Piątkowski, M., Bogdał, D., "Coumarin-Modified CQDs for Biomedical Applications—Two-Step Synthesis and Characterization" *Int. J. Mol. Sci.* 2020, **21**, 8073.
48. Feng, Z., Li, Z., Zhang, X., Xu, G., Zhou, N., "Fluorescent carbon dots with two absorption bands: luminescence mechanism and ion detection" *J. Mater. Sci.* 2018, **53**, 6459-6470.
49. Ionita, P., "Is DPPH stable free radical a good scavenger for oxygen active species?" *Chem. Pap.* 2005, **59**, 11-16.
50. Zhang, J., Wang, X., Vikash, V., Ye, Q., Wu, D., Liu, Y., Dong, W., "ROS and ROS-mediated cellular signaling" *Oxid. Med. Cell. Longev.* 2016, **2016**.
51. Shields, H.J., Traa, A., Van Raamsdonk, J.M., "Beneficial and detrimental effects of reactive oxygen species on lifespan: A comprehensive review of comparative and experimental studies" *Front. Cell Dev. Biol.* 2021, **9**, 181.
52. Alfadda, A.A.,Sallam, R.M., "Reactive oxygen species in health and disease" *J. Biomed. Biotechnol.* 2012, **2012**.
53. Réblová, Z., "Effect of temperature on the antioxidant activity of phenolic acids" *Czech J. Food Sci.* 2012, **30**, 171-175.
54. Zhang, Y., Wang, Y., Feng, X., Zhang, F., Yang, Y., Liu, X., "Effect of reaction temperature on structure and fluorescence properties of nitrogen-doped carbon dots" *Appl. Surf. Sci.* 2016, **387**, 1236-1246.
55. Chunduri, L., Kurdekar, A., Patnaik, S., Dev, B.V., Rattan, T.M., Kamisetti, V.J.M.F., "Carbon quantum dots from coconut husk: evaluation for antioxidant and cytotoxic activity" 2016, **5**, 55-61.
56. Sarkar, S., Banerjee, D., Ghorai, U.K., Das, N.S., Chattopadhyay, K.K., "Size dependent photoluminescence property of hydrothermally synthesized crystalline carbon quantum dots" *J. Lumin.* 2016, **178**, 314-323.
57. Al Mamari, H.H., *Phenolic Compounds: Classification, Chemistry, and Updated Techniques of Analysis and Synthesis*, in *phenolic Compounds*. 2021, IntechOpen.
58. Miklasińska-Majdanik, M., Kępa, M., Wojtyczka, R.D., Idzik, D., Wąsik, T.J., "Phenolic compounds diminish antibiotic resistance of Staphylococcus aureus clinical strains" *Int. J. Environ. Res.* 2018, **15**, 2321.
59. Egorov, A., Ulyashova, M., Rubtsova, M.Y., "Bacterial enzymes and antibiotic resistance" *Acta Naturae* 2018, **10**, 33-48.
60. Zhao, C., Wang, X., Wu, L., Wu, W., Zheng, Y., Lin, L., Weng, S., Lin, X.J.C., Biointerfaces, S.B., "Nitrogen-doped carbon quantum dots as an antimicrobial agent against Staphylococcus for the treatment of infected wounds" 2019, **179**, 17-27.
61. Hajipour, M.J., Fromm, K.M., Ashkarran, A.A., de Aberasturi, D.J., de Larramendi, I.R., Rojo, T., Serpooshan, V., Parak, W.J., Mahmoudi, M.J.T.i.b., "Antibacterial properties of nanoparticles" 2012, **30**, 499-511.
62. Wu, Y., Li, C., van der Mei, H.C., Busscher, H.J., Ren, Y., "Carbon Quantum Dots Derived from Different Carbon Sources for Antibacterial Applications" *Antibiotics (Basel)* 2021, **10**, 623.
63. de Almeida, C.G., Garbois, G.D., Amaral, L.M., Diniz, C.C., Le Hyaric, M., "Relationship between structure and antibacterial activity of lipophilic N-acyldiamines" *Biomed. Pharmacother* 2010, **64**, 287-290.